Chemo-Mechanical Coupling in the Rotary Molecular Motor F_1-ATPase

Kengo Adachi,[1] Shou Furuike,[1] Mohammad Delawar Hossain,[1,2] Hiroyasu Itoh,[3] Kazuhiko Kinosita, Jr.,[1*] Yasuhiro Onoue,[1,4] and Rieko Shimo-Kon[1]

[1]Department of Physics, Faculty of Science and Engineering, Waseda University, Okubo, Shinjuku-ku, Tokyo 169-8555, Japan.

[2]Department of Physics, School of Physical Sciences, Shahjalal University of Science and Technology, Sylhet-3114, Bangladesh.

[3]Tsukuba Research Laboratory, Hamamatsu Photonics KK, Tokodai, Tsukuba 300-2635, Japan.

[4]Department of Functional Molecular Science, The Graduate University for Advanced Studies (Sokendai), Okazaki, Aichi 444-8585, Japan

[*]Correspondence: kazuhiko@waseda.jp http://www.k2.phys.waseda.ac.jp

Abstract F_1-ATPase is a molecular motor in which the central γ subunit rotates inside the cylinder made of $\alpha_3\beta_3$ subunits. The rotation is powered by ATP hydrolysis in three catalytic sites, and reverse rotation of the γ subunit by an external force leads to ATP synthesis in the catalytic sites. Single-molecule studies have revealed how the mechanical rotation is coupled to the chemical reactions in the three catalytic site: binding/release of ATP, ADP, and phosphate, and hydrolysis/synthesis of ATP.

1. Introduction

F_1-ATPase, a water-soluble portion of ATP synthase, has been predicted (Boyer and Kohlbrenner, 1981; Oosawa and Hayashi, 1986) and proved (Noji et al., 1997) to be an ATP-driven rotary molecular motor in which the central γ subunit rotates inside a hexameric cylinder made of alternately arranged three α and three β subunits (Abrahams et al., 1994). When the rotor subunit γ is rotated in reverse by application of an external force, the motor turns into a generator and synthesizes ATP from ADP and inorganic phosphate (Pi) in the catalytic sites (Itoh et al., 2004; Rondelez et al., 2005). F_1 is thus a reversible chemo-mechanical energy converter as its physiological role implies (Boyer, 1997; Yoshida et al., 2001; Kinosita et al., 2000a, 2000b, 2004).

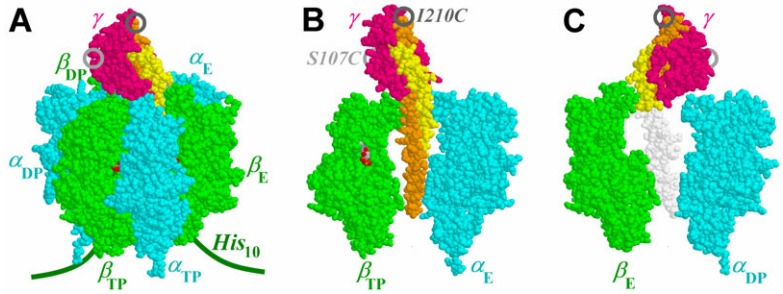

Fig. 1. A crystal structure (Gibbons et al., 2000) of mitochondrial F_1 (MF_1). α and β subunits are designated according to the nucleotides in catalytic sites found in the original structure (Abrahams et al., 1994): TP site between β_{TP} and α_{TP}, largely in β_{TP}, bound an ATP analog, DP site ADP, and E site none, while non-catalytic sites in the other three interfaces bound the ATP analog. TF_1 that we use has a similar structure (Shirakihara et al., 1997), to which we introduced two cysteines on γ (circles) and ten histidines at the N-terminus of β. N- and C-terminal α-helices of the γ subunit are shown in yellow and orange, respectively. Nucleotides are in CPK colors. (A) An overall view. (B) A side view showing an opposing α-β pair. (C) An "axle-less" construct in which the white portion was deleted (Furuike et al., 2008a).

We have been working on F_1 of thermophilic origin (TF_1) for about ten years, during which our views about its rotary mechanism have changed significantly. We have been, and still are, seeking for the simplest interpretations of existing data, but Nature seems not always simple. Here we present our current views, together with critical evaluations of our work to help the reader make his/her own judgments.

2. Rotation Scheme

We observe rotation under an optical microscope by attaching β subunits of F_1 to a glass surface through the engineered histidine tags (Fig. 1A). Sole two cysteines in our TF_1 (only S107C in early studies) on the protruding portion of γ (Fig. 1) are biotinylated, to which a probe for imaging γ rotation, a micron-sized actin filament (Noji et al., 1997) or a spherical bead (or its duplex) with a size 1 μm down to 40 nm is attached through biotin-avidin linkage.

2.1 Data Selection

We typically infuse ~0.1 nM of F_1 into an observation chamber of height ~50 μm. If all are attached, the surface density would be of the order of 1 molecule/μm^2. In fact, only on lucky days do we observe as many as tens of rotating probes in a field of view some (300 $\mu m)^2$. Most of the motors are inactive, or fail to bind the probe, which is huge compared to the motor size of ~10 nm, in a configuration

that allows unhindered rotation. Of those that rotate, we select those few that rotate fast, smooth, and with 120° symmetry (see below). Due to this subjective selection, ensemble statistics in our work is unreliable, though we make every effort at increasing the number of selected to convince ourselves that we are not reporting artifacts. Our statistics relies on repeated behaviors of a selected molecule: we analyze many consecutive revolutions without eliminating an event in the sequence.

2.2 120° Step per ATP

When ATP concentration, [ATP], is low, the rotation proceeds in steps of 120°, with stepping frequency proportional to [ATP] (Yasuda et al., 1998). This indicates a 120° step per ATP hydrolyzed, as expected from the presence of three basically equivalent catalytic sites. Bulk rate of ATP hydrolysis, however, has always been somewhat lower than the stepping rate under a negligible load (Yasuda et al., 2001). Our explanation is that part of F_1 in bulk solution is inhibited or less active in some way, but other interpretations cannot be excluded. F_1 is known to be inhibited when it binds MgADP tightly (Jault et al., 1996; Hirono-Hara et al., 2001). We thus prepare nucleotide-free F_1 (Noji et al., 2001; Adachi et al., 2003), but ADP is formed during catalysis. Phosphoenolpyruvate used in ATPase assay has been found to be a competitive inhibitor (R. Shimo-Kon, unpublished).

2.3 Substeps

With a 40-nm gold bead for which viscous friction is not too high, the 120° step is further resolved into 80-90° and 40-30° substeps (Yasuda et al., 2001; Adachi et al., 2007), which we refer to here as 80° and 40° (see Fig. 2A below). The substep behavior can be resolved only in selected molecules, and those selected do not necessarily show substeps in the entire time course observed. But we have seen many examples where a molecule shows several hundreds of consecutive substeps, and thus we regard this a genuine property of F_1. We notice momentary pauses in other angles under certain conditions, but we are much less certain if these are also genuine.

2.4 Direction of Rotation

In all cases the direction of ATP-driven rotation is counterclockwise when viewed from above in Fig. 1. It is actually mere presumption that in all rotating molecules the His-tags are attached to the glass surface. Indeed, rotation can be observed on a clean glass surface (Yasuda et al., 2001), without functionalizing the surface

with Ni-NTA that is supposed to bind histidine specifically. In no experiment is there guarantee that all three His-tags are bound tightly on a surface. Sometimes the positions of ATP-waiting angles separated by 120° shift during the course of observation, suggesting detachment and reattachment of a His-tag(s). When we manipulate the γ angle by magnets (Adachi et al., 2007), therefore, we confirm the ATP-waiting angles both before and after a measurement by infusing nanomolar ATP and let the F_1 undergo spontaneous stepping rotation (a laborious and often irritating procedure). Also, a probe such as a plastic bead can attach to γ by non-specific binding. There are cases, though rare, where we believe that γ is attached to a glass surface and a probe on the $\alpha_3\beta_3$ cylinder. The sense of rotation, though, remains counterclockwise even in this upside down configuration.

We strive to make objective selection of data and to report 'facts,' but we are too aware that a fact 'described' by words is no longer a fact and, worse, that we often make false judgments.

3. Chemo-Mechanical Coupling

Here we discuss the relation between the rotary angle of γ and chemical reactions in the three catalytic sites. ATP synthesis by manipulation of the γ angle alone suggests a γ-dictator mechanism where the state of the motor, or rather the probability a state is realized, is determined basically by one parameter, the γ angle (in addition to environmental variables such as [ATP]). For simplicity, we assume that this holds to a first approximation. We also simplify chemical kinetics and decompose it into the minimum of four pairs of events, binding and release of ATP, ADP, and Pi, and hydrolysis and synthesis of ATP.

3.1 ATP Binding

In Fig. 2A we show schematically a rotation time course involving substeps. The duration of ATP-waiting dwells, on multiples of 120° in Fig. 2A, is inversely proportional to [ATP] below K_m of about 15 μM down to nM (Sakaki et al., 2005) for wild-type TF_1, and become negligibly short (≤0.1 ms) at saturating [ATP]s. Because the 80° substep that follows is complete in 0.1 ms, short on the time scale of protein functions, we proposed that the 80° rotation is not only triggered but also driven (powered) all the way by ATP binding (Yasuda et al., 2001). A later study (Adachi et al., 2007), however, has indicated that ADP release also occurs during the 80° substep and that ADP release would also drive the substep (see below).

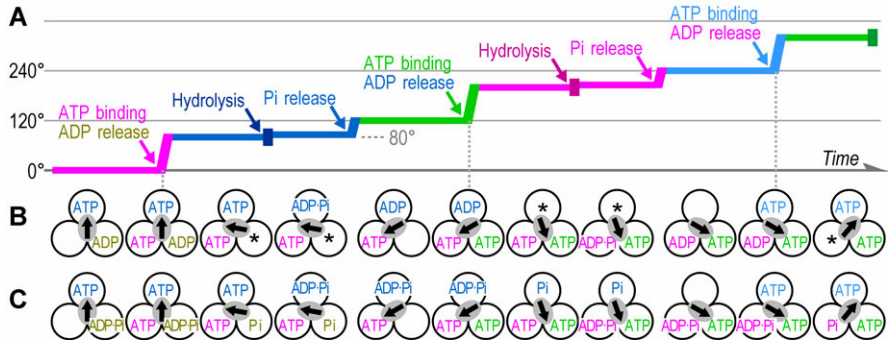

Fig. 2. Proposed scheme for coupling between catalysis and rotation. (**A**) Schematic time course of rotation. Colors indicate the site at which the rate-limiting reaction is to occur in B. (**B** and **C**) Alternative schemes suggested by Adachi et al. (2007), differing in the timing of Pi release by 120°. Chemical states of three catalytic sites (circles) and γ orientation (central arrows) are shown. More recent work (R. Shimo-Kon, unpublished) points to B, where the empty site with an asterisk is freely accessible to medium nucleotides.

3.2 Hydrolysis of ATP

Histograms of the dwell times at 80° indicate that at least two reactions take place at 80° (Yasuda et al., 2001). One is likely ATP hydrolysis, because the 80° dwell becomes longer in the β-E190D mutant in which a glutamate presumed to attack the terminal phosphate is replaced with aspartate, or when the medium contained ATP-γ-S that is presumably hydrolyzed slowly (Shimabukuro et al., 2003). Cy3-ATP, a fluorescent analog of ATP, also prolongs the 80° dwell when the Cy3-ATP is bound 200° ago (Nishizaka et al., 2004), suggesting that binding of ATP and cleavage of that ATP is separated by 200° (see, e.g., the fate of pink ATP in Fig. 2). The β-E190D mutant also points to this scenario (Ariga et al., 2007). The evidence, though, is not perfect in that hydrolysis has not been confirmed directly.

Oxygen exchange studies by Boyer and colleagues have shown that, at low [ATP]s, bound ATP undergoes rounds of reversible hydrolysis/re-synthesis before ADP and Pi are eventually released into the medium (O'Neal and Boyer, 1984; Boyer, 1997). The reversals must occur at ATP-waiting angles, possibly accompanying angular fluctuations of γ. In our scheme in Fig. 2, it is the cyan 'ATP' at 0° that would undergo reversible hydrolysis. The reversals would be biased toward synthesis at 0° but almost completely toward hydrolysis at 80°. Whether the rate-limiting step at 80° is merely this shift in equilibrium or a process that somehow ensures completion of hydrolysis, e.g., movement of an 'arginine finger' in the catalytic site (Kagawa et al., 2004), is not known. An unexpected finding that the long dwell at 80° in the β-E190D mutant disappears when the preceding ATP-

waiting dwell at 0° is long (seconds) suggests that the reversals may end in hydrolysis at 0° by subsequent Pi release if sufficient number of reversal are allowed (Shimabukuro et al., 2006).

For efficient ATP synthesis in cells, coupling between rotation and hydrolysis is advantageous because, then, reverse rotation of γ will ensure ATP synthesis (Kinosita et al., 2004). This is fulfilled if the shift in equilibrium from predominantly ATP to predominantly ADP+Pi occurs over the 80° rotation, but then the nature of the slow reaction at 80° observed with ATP-γ-S, Cy3-ATP, or β-E190D is unclear. Or, the shift begins after γ has rotated into the 80° position and may accompany a small amount of further rotation, e.g., from 80° to 90°. In this regard, we note that substep angle close to 80° has been observed in situations where hydrolysis reaction is presumed to be slow (ATP-γ-S, Cy3-ATP, β-E190D), whereas high-speed (and thus noisy) observation of normal rotation is compatible with any angle around 80-90° (Yasuda et al., 2001; Adachi et al., 2007).

3.3 Pi Release

Another event at 80° interim is Pi release (Adachi et al., 2007): medium Pi specifically prolongs the 80° dwell, indicating that Pi release at least triggers the next 40° substep. Furthermore, with Pi at hundreds of millimolar, frequent reversals of 40° substeps are observed, showing that Pi release drives the 40° rotation. Two possibilities, however, have remained for the timing of Pi release: either immediately after hydrolysis (Fig. 2B) or after further 120° of rotation (Fig. 2C). Our recent work (R. Shimo-Kon, unpublished) suggests that the site indicated by an asterisk in Fig. 2B is accessible to medium nucleotides including ATP, and that medium Pi competes with the nucleotide binding. Thus, Fig. 2C where this site is occupied by catalytic Pi (Pi formed by ATP hydrolysis) is unlikely.

The analysis of 80° dwells by itself indicates only the presence of two (or more) rate-limiting reactions, which may be sequential or parallel (but both must complete before the next 40° substep). The Pi results above indicate that hydrolysis (with the reservations in 3.2) and Pi release occur in the same site in this order, taking ~0.2 ms and ~1.2 ms, respectively, at room temperature (Adachi et al., 2007). Involvement of another reaction(s), however, cannot be excluded.

3.4 ADP Release

Initially we suggested, without evidence, that the 40° substep is likely driven by ADP release that occurs after 200° of rotation since that ADP was bound as ATP at 0°. We were influenced by the crystal structures that show hinge bending of ~30° in β_{TP} or β_{DP} compared to β_E (Fig. 1): if the 80° substep is driven by ATP

binding that would bend a β, then the rest of 40° rotation would likely be driven by ADP release that should unbend the β (Wang and Oster, 1998). We also thought, in those days, that the site occupancy, the number of catalytic sites occupied by a nucleotide, would alternate between one and two (see below), and hence ADP should be released before 240° of rotation.

Imaging of binding and release of Cy3-ATP (Nishizaka et al., 2004), however, showed that the fluorescent nucleotide remains on a mutant F_1 for at least 240° of rotation. Precise timing of (Cy3-)ADP release could not be determine, but it must have been between 240° and 360°. Later, retention of Cy3-AT(D)P for ≥240° was confirmed with wild-type F_1: when rotation was artificially slowed by magnets, release occurred at ~240°, and, in free rotation under the conditions where the 80° dwells were long (β-E190D or in the presence of ATP-γ-S), release occurred between 240° and 320° (Adachi et al., 2007). Practical temporal resolution in these measurements, however, was ~0.1 s, and thus, in normal rotation where the 80° dwells take only 1-2 ms, release may be delayed until the end of the 320° dwell or even beyond 320° (but certainly not beyond 360°). Also, there is no guarantee that Cy3-ATP behaves in the same way as unlabeled ATP, and thus, until recently, we thought that unlabeled ADP might be released before 240°.

Now we think that release of unlabeled ADP occurs within ~1 ms from the start of the substep from 240° to 320°: either during the substep rotation or in an early part of the dwell at 320°. Evidence comes from the site occupancy study below.

3.5 Site Occupancy

Rotation in one direction requires broken symmetry. Because the crystal structures suggested a conformational change of the β subunits (bending/unbending) that depends on the presence or absence of a bound nucleotide, we thought that bi-site catalysis which would warrant maximal asymmetry (in terms of the occupancy of the three catalytic sites) would be the natural choice (Kinosita et al., 2000a, 2000b). Studies on MF_1 also indicated bi-site catalysis (Milgrom and Cross, 2005, and references therein).

Senior and colleagues have introduced a reporter tryptophan in the catalytic sites of *Escherichia-coli* F_1 (EF_1) and directly measured the site occupancy. They have shown that the ATP hydrolysis activity parallels the occupancy of the third site, implicating a tri-site mechanism where the site occupancy alternates between two and three, being three during the rate-limiting step of the catalysis (Weber et al., 1993; Weber and Senior, 2000). Studies on TF_1 basically corroborated the results (Dou et al., 1998; Ono et al., 2003).

Our recent work using a reporter tryptophan in a mutant TF_1 (R. Shimo-Kon et al., unpublished) has also shown that the occupancy rises to three as [ATP] increases. The rise, however, is preceded by the rise in hydrolysis activity: at the [ATP] where the activity is half maximal (K_m), the occupancy is only slightly

above two. At K_m, F_1 spends half of its time at the 0° (ATP-waiting) position and the other half at 80° (Fig. 2). For the time-averaged occupancy to be close to two, ADP has to be released during the 80° substep or immediately (well within the 80° dwell time of ~2 ms) after the 80° rotation. At [ATP] >> K_m, the asterisked vacated site in Fig. 2 can bind medium nucleotide weakly, allowing the occupancy to rise to three. The study has also shown that, at least for the particular mutant studied, bi-site activity is virtually absent.

4. Energetics of Coupling

Our view here is that the free-energy drops in the chemical reactions, ATP binding, hydrolysis, Pi release and ADP release, drive rotation (Kinosita et al., 2004). Some of these partial reactions may be uphill, depending on the ligand concentrations in the medium and the load if present, but the rotation goes counterclockwise as long as the overall free-energy drop is greater than the mechanical work F_1 has to do against a conservative load (such as a spring). For the process of Pi release, the energetics has been worked out (Adachi et al., 2007).

4.1 Pi Release

From high-speed imaging of unloaded rotation at various [Pi], we have determined the rate constants for Pi release and Pi rebinding at 80° and 120° (vertical arrows in Fig. 3B) and rotation between these angles (oblique arrows). The rate constants in turn allow us to calculate free energy levels as shown in Fig. 3B. The free energy for a given chemical state (F_1·ADP·Pi representing the state still binding the Pi to be released, or F_1·ADP obtained after Pi release) must be a function of rotary angle, as in the simplified linear diagram in Fig. 3A. For the analysis, however, we chose the two-state approximation in Fig. 3B to determine a minimal number of rate constants.

Solid horizontal bars in Fig. 3B show energy levels at 50 mM Pi. At this [Pi], release of Pi at 80° is mostly unsuccessful because rebinding rate is high. Once in about ten release events, though, the F_1·ADP formed by Pi release rotates into the 120° conformation, where the probability of Pi rebinding is extremely low and thus F_1·ADP is stable. At 5 mM Pi (dashed lines), Pi release at 80° is easier. At 500 mM Pi, on the other hand, the energy levels for F_1·ADP are shifted upward, leading to a finite probability of Pi rebinding at 120° followed by rotation back to 80°, as was experimentally observed (Adachi et al., 2007).

The dissociation constant for Pi, K_d^{Pi}, is calculated from the rate constants to be 4.9 mM at 80° and ~200 M at 120°, implying >10^4-fold reduction in the affinity for Pi upon rotation from 80° to 120°. K_d^{Pi}(80°) of 4.9 mM is close to physiologi-

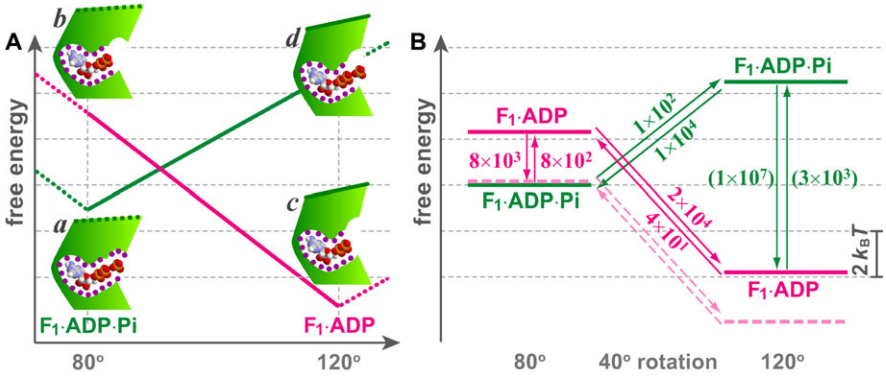

Fig. 3. Free-energy diagrams for the 40° rotation accompanying Pi release (Adachi et al., 2007). (**A**) Simplified potential energies for the rotation of γ in the state F_1·ADP·Pi before Pi release and in F_1·ADP after Pi release (green and magenta lines, respectively). The lines show, very approximately, how the free energy of the system changes when γ is rotated while the chemical state is fixed (see Kinosita et al., 2004). The green blocks *a*-*d* are schematic representations of the two conformations (80° and 120°) of F_1 and the catalytic site from which Pi is released. ADP and Pi are shown in space filling models. Small violet dots represent interactions (mainly hydrogen bonds) through which the protein part (green) and the ligands attract each other. (**B**) Two-state approximation of the angle dependent free energies in (A). Four energy levels (horizontal bars) are considered for given [Pi], and the transition rates (in s^{-1}) have been determined from experiments, except for the parenthesized numbers for which only their ratio is experimental (Adachi et al., 2007). Solid lines with numerical values are for 50 mM Pi. Dashed lines are for 5 mM Pi. Diagrams for other [Pi] can be obtained by shifting the magenta bars vertically in proportion to k_BT·ln[Pi] where k_BT = 4.1 pN·nm is the thermal energy at room temperature. Only the rates of Pi binding change with [Pi].

cal [Pi], but this rather low affinity is due to the two-state approximation. Actual K_d^{Pi}(80°) in the angle-dependent diagram (Fig. 3A) will be smaller, assuring efficient Pi binding during ATP synthesis by reverse rotation.

If Pi release drives rotation from 80° to 120°, then rotation from 80° to 120°, whether spontaneous or by an external force, must accompany a reduction in the affinity for Pi. This is the law of action and reaction, proved for this case by experiment above. Cartoons in Fig. 3A illustrate this, where the green blocks represent protein part and space filling models ADP and Pi. In *a*, Pi, together with ADP, pulls the protein towards itself. When Pi leaves (*b*), the pulling force reduces and then the protein springs back to a less bent (relaxed) conformation (*c*). In this conformation, the affinity for Pi is low, because bond formation is difficult due to the widening of the catalytic site (*d*). If we start from *d*, the transition toward *a* is a process of 'induced fit' (Koshland, 1958) where the catalytic site, and hence the protein as a whole, adapts their conformations to tightly accommodate the bound Pi. The protein and the ligand pull each other, observing the law of action and reaction. The reverse of this process may be called 'induced unfit.'

4.2 Power Stroke versus Diffusion and Catch

The term induced fit apparently implies that ligand binding is the cause of protein conformational change (Fig. 3A $c \rightarrow d \rightarrow a$). In fact, the protein conformation fluctuates thermally, and thus one can expect, when the protein adopts thermally a conformation suitable for binding, the ligand binds and stabilizes that conformation ('conformational selection'). In this latter process ($c \rightarrow b \rightarrow a$), conformational change is apparently the cause of binding. As long as one compares the start (c) and end (a), however, the two processes are equivalent: either ligand binding or conformational change can be the cause of the other. The two processes are distinguished only kinetically (through d or through b).

The equivalent of induced fit versus conformational selection for the case of a motor protein is power stroke (a force-generating conformational change driven by a chemical reaction) versus diffusion and catch (thermal fluctuation, even against an external force, followed by stabilization by chemical reaction). As we have discussed above, the distinction is meaningful only kinetically. For protein machines, the energy involved is not much greater than the thermal energy, and hence one cannot expect that one of the two processes overwhelms the other.

Furthermore, the two processes likely cooperate with each other. The seesaw energy diagram in Fig. 3A (the linear angle dependence is simplification) indicates that forward (from 80° to 120°) fluctuation in the state F_1·ADP·Pi will decrease the affinity for Pi and thus assist Pi release, and that, once Pi is released, the downhill slope in F_1·ADP will assist forward rather than backward fluctuations. Power stroke versus diffusion and catch is more of conceptual distinction rather than practical.

In our analysis of the 40° substep by Pi release, we presumed for simplicity the power stroke ($a \rightarrow b \rightarrow c$) scenario rather than diffusion and catch ($a \rightarrow d \rightarrow c$). The energy levels we arrived at (Fig. 3B) are consistent with this assumption, but this does not imply that the power stroke view is correct.

4.3 Chemo-Mechanical Coupling by Induced Fit and Unfit

We think that protein (or RNA) machines that convert free energy of chemical reactions into mechanical work operate by a series of induced fit and induced unfit (Fig. 4). Here we define fit and unfit in a broad sense and do not distinguish them from conformational selection (we discuss energetics rather than kinetics).

In the case of F_1, all reactions toward right (overall hydrolysis) are likely downhill under the laboratory conditions of high [ATP] and low [ADP] and [Pi], except for the hydrolysis step for which the energy involved may be small (Kinosita et al., 2004). Counterclockwise rotation under these conditions are smooth and fast, exceeding 700 revolutions s^{-1} for TF_1 at high temperatures (Furuike et al., 2008b).

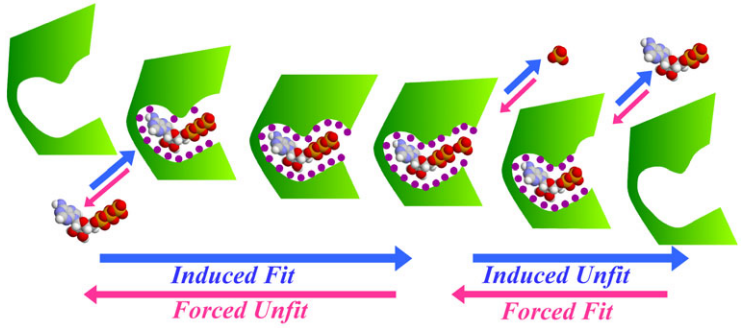

Fig. 4. Chemo-mechanical and mechano-chemical energy conversion through a series of fitting and unfitting processes. Blue arrows, reaction driven by free energy of hydrolysis; pink arrows, reverse reactions driven by an external force.

F_1-ATPase is a reversible molecular machine (Itoh et al., 2004). ATP synthesis by clockwise rotation driven by an external force would proceed as a series of forced fit and unfit (Fig. 4). Whether synthesis follows the hydrolysis pathway (Fig. 2B) precisely in reverse is yet to be clarified.

5. Structural basis of rotation

The relation between chemical reactions and rotation has basically been worked out. The scheme in Fig. 2B may apply only to TF_1, or the scheme may turn out to be wrong in its details. There is, however, one coupling scheme (Fig. 2B) that we can propose, at least as a working hypothesis. For the structural changes underlying rotation, in contrast, we cannot propose, at present, even a possible mechanism. We thought that the push-pull mechanism suggested by Wang and Oster (1998) was reasonable, but it is at best part of the actual mechanism (see below).

5.1 Crystal structures

Walker and colleagues have solved many crystal structures of F_1 (mostly MF_1) that have served as the basis for the understanding of the mechanism of catalysis and also for designing experiments including single-molecule studies. Important differences among the crystals have been found in the catalytic sites, but overall structures closely resemble each other, except for one in which all three catalytic sites are filled with a nucleotide and β_E adopts a different shape (Menz et al., 2001). All others bind two catalytic nucleotides, as in our coupling scheme (Fig. 2B), and one catalytic site is widely open. Even in the structure with three cata-

lytic sites filled, subunits other than β_E adopted configurations similar to those in other crystals.

Many of the crystals were prepared in the presence of azide, which is known to enhance the MgADP inhibition (Jault et al., 1996), and azide has been resolved in a crystal (Bowler et al., 2006). Thus, the mutually similar structures, including that of EF_1 (Hausrath et al., 2001) which was also prepared in the presence of azide, must all represent, basically, the MgADP-inhibited state. In this state, γ is orientated at 80° (Hirono-Hara et al., 2001), as in the 80° intermediate during active rotation. Fluorescence energy transfer between probes on a β and rotating γ has indicated that, of the two active rotation intermediates at 0° and 80°, the crystal structures are much closer to the 80° intermediate (Yasuda et al., 2003). At 80°, we expect one catalytic site to be open to the medium (asterisks in Fig. 2B), which is consistent with the idea that the crystal structures with a fully open catalytic site mimic the 80° state rather than the ATP-waiting state.

The crystal structures show that the γ axle can be twisted around its axis. The bottom tip (of the longer C-terminal helix) does not differ much among the crystals, but, in the orifice region, the γ coiled coil in the three-nucleotide structure (Menz et al., 2001) is twisted clockwise by ~20° relative to the original structure (Abrahams et al., 1994). In a yeast MF_1 structure (Kabaleeswaran et al., 2006), on the other hand, γ is rotated ~12° counterclockwise relative to the original structure; the latter could be due to species difference, but other two molecules in the same unit cell show clockwise, rather than counterclockwise, twists.

The twist in the three-nucleotide structure is opposite to the rotational direction, suggesting that the third nucleotide in the β_E site (ADP) may correspond to the leaving ADP in our scheme (gold in Fig. 2B). The tip of β_E that touches γ in the orifice region of this structure is rotated ~16° counterclockwise (Menz et al., 2001) relative to the original structure, as though the β tip is preventing counterclockwise rotation of γ until the ADP leaves and the β tip retracts. The twist in γ, however, could be due to lattice contacts, because clockwise twist of ~11° was also seen in the structure in Fig. 1 where one catalytic site is open.

5.2 Axle-less constructs

As seen in Fig. 1, β_{TP} and β_{DP} (with an overall structure very similar to β_{TP}) are bent toward, and apparently push, the top of the γ axle, whereas β_E retracts and pulls γ. The combined actions could rotate the slightly bent and skewed axle while the lower tip of the axle is held relatively stationary by the $\alpha_3\beta_3$ cylinder (Wang and Oster, 1998). Though this view was attractive, we have recently found that an axle-less mutant (Fig. 1C) can rotate in the correct direction for >100 revolutions (Furuike et al., 2008a). Neither a rigid axle nor a fixed support at the bottom, essential to the push-pull mechanism, is necessary for rotation. At present,

we do not understand how this axle-less construct rotates and how the γ head that apparently sits on the concave stator orifice can stay attached while undergoing many revolutions. The twist of γ seen in some crystals suggests torque generation in the orifice region alone, if it is not an artifact resulting from lattice contacts.

As we truncate the γ axle from the tip step by step, the bulk hydrolysis activity gradually diminishes, whereas the apparent torque becomes ~half that of the wild type at the C-terminal truncation nearly level with the N-terminus and thereafter remains constant (Hossain et al., 2006, 2008). It appears that a rigid axle and bottom support are needed for high-speed catalysis and generation of full torque, but orifice interactions alone can produce half the torque.

6. Remaining Tasks

To relate structure and function in F_1-ATPase, we need at least one more crystal structure that is grossly different from others, hopefully one that mimics the ATP-waiting state. Torque of this motor, so far inferred from the viscous friction against a probe attached to γ, needs to be better characterized. The best is to measure the stall torque against a conservative external torque, at all γ angles for each chemical state of F_1, to construct the potential energy diagram as in Fig. 3A for all angles and for all states. This is a formidable task, but we are still trying. ATP synthesis by reverse rotation is poorly understood. We are yet to learn, for example, at which angles ADP and Pi are picked up from the medium and when ATP is released; whether and to what extent the forced γ rotation is blocked until the expected chemical reaction has taken place. A lot remain to be clarified, even for this relatively well-understood molecular machine.

Acknowledgments We thank members of Kinosita and Yoshida labs for collaboration and discussion, R. Kanda-Terada for technical support, K. Sakamaki, M. Fukatsu and H. Umezawa for encouragement and lab management. This work was supported by Grants-in-Aids for Specially Promoted Research from the Ministry of Education, Sports, Culture, Science and Technology, Japan.

References

Abrahams, J. P., Leslie, A. G. W., Lutter, R., and Walker, J. E. (1994). Structure at 2.8Å resolution of F_1-ATPase from bovine heart mitochondria. *Nature* **370**, 621–628.

Adachi, K., Noji, H., and Kinosita, K., Jr. (2003). Single-molecule imaging of rotation of F_1-ATPase. *Methods Enzymol.* **361**, 211-227.

Adachi, K., Oiwa, K., Nishizaka, T., Furuike, S., Noji, H., Itoh, H., Yoshida, M., and Kinosita, K., Jr. (2007). Coupling of rotation and catalysis in F_1-ATPase revealed by single-molecule imaging and manipulation. *Cell* **130**, 309-321.

Ariga, T., Muneyuki, E., and Yoshida, M. (2007). F_1-ATPase rotates by an asymmetric, sequential mechanism using all three catalytic subunits. *Nat. Struct. Mol. Biol.* **14**, 841-846.

Bowler, M. W., Montgomery, M. G., Leslie, A. G. W., and Walker, J. E. (2006). How azide inhibits ATP hydrolysis by the F-ATPases. *Proc. Natl. Acad. Sci. USA* **103**, 8646-8649.

Boyer, P.D. (1997). The ATP synthase — a splendid molecular machine. *Annu. Rev. Biochem.* **66**, 717-749.

Boyer, P. D., and Kohlbrenner, W. E. (1981). The present status of the binding-change mechanism and its relation to ATP formation by chloroplasts. *In* Energy coupling in photosynthesis, B.R. Selman and S. Selman-Reimer, eds. (Amsterdam: Elsevier), pp. 231-240.

Dou, C., Fortes, P. A. G., and Allison, W. S. (1998). The $\alpha_3(\beta Y341W)_3\gamma$ subcomplex of the F_1-ATPase from the Thermophilic *Bacillus* PS3 fails to dissociate ADP when MgATP is hydrolyzed at a single catalytic site and attains maximal velocity when three catalytic sites are saturated with MgATP. *Biochemistry* **37**, 16757-16764.

Furuike, S., Hossain, M. D., Maki, Y., Adachi, K., Suzuki, T., Kohori, A., Itoh, H., Yoshida, M., and Kinosita, K., Jr. (2008a). Axle-less F_1-ATPase rotates in the correct direction. *Science* **319**, 955-958.

Furuike, S., Adachi, K., Sakaki, N., Shimo-Kon, R., Itoh, H., Muneyuki, E., Yoshida, M., and Kinosita, K., Jr. (2008b). Temperature dependence of the rotation and hydrolysis activities of F_1-ATPase. *Biophys. J.* **95**, 761-770.

Gibbons, C., Montgomery, M. G., Leslie, A. G. W., and Walker, J. E. (2000). The structure of the central stalk in bovine F_1-ATPase at 2.4Å resolution. *Nat. Struct. Biol.* **7**, 1055-1061.

Hausrath, A. C., Capaldi, R. A., and Matthews, B. W. (2001). The conformation of the ε- and γ-subunits within the *Escherichia coli* F_1 ATPase. *J. Biol. Chem.* **276**, 47227-47232.

Hirono-Hara, Y., Noji, H., Nishiura, M., Muneyuki, E., Hara, K. Y., Yasuda, R., Kinosita, K., Jr. and Yoshida, M. (2001). Pause and rotation of F_1-ATPase during catalysis. *Proc. Natl. Acad. Sci. USA* **98**, 13649–13654.

Hossain, M. D., Furuike, S., Maki, Y., Adachi, K., Ali, M. Y., Huq, M., Itoh, H., Yoshida, M., and Kinosita, K. Jr. (2006). The rotor tip inside a bearing of a thermophilic F_1-ATPase is dispensable for torque generation. *Biophys. J.* **90**, 4195-4203.

Hossain, M. D., Furuike, S., Maki, Y., Adachi, K., Suzuki, T., Kohori, A., Itoh, H., Yoshida, M., and Kinosita, K. Jr. (2008). Neither helix in the coiled coil region of the axle of F_1-ATPase plays a significant role in torque production. *Biophys. J.* **95**, 4837-4844.

Itoh, H., Takahashi, A., Adachi, K., Noji, H., Yasuda, R., Yoshida, M., and Kinosita, K., Jr. (2004). Mechanically driven ATP synthesis by F_1-ATPase. *Nature* **427**, 465-468.

Jault, J. M., Dou, C., Grodsky, N. B., Matsui, T., Yoshida, M., and Allison, W. S. (1996). The $\alpha_3\beta_3\gamma$ subcomplex of the F_1-ATPase from the thermophilic *Bacillus* PS3 with the βT165S substitution does not entrap inhibitory MgADP in a catalytic site during turnover. *J. Biol. Chem.* **271**, 28818–28824.

Kabaleeswaran, V., Puri, N., Walker, J. E., Leslie, A. G. W., and Mueller, D. M. (2006). Novel features of the rotary catalytic mechanism revealed in the structure of yeast F_1 ATPase. *EMBO J.* **25**, 5433-5442.

Kagawa, R., Montgomery, M. G., Braig, K., Leslie, A. G. W., and Walker, J. E. (2004). The structure of bovine F_1-ATPase inhibited by ADP and beryllium fluoride. *EMBO J.* **23**, 2734-2744.

Kinosita, K., Jr., Yasuda, R., and Noji, H. (2000a). F_1-ATPase: a highly efficient rotary ATP machine. *Essays Biochem.* **35**, 3-18.

Kinosita, K., Jr., Yasuda, R., Noji, H., and Adachi, K. (2000b). A rotary molecular motor that can work at near 100% efficiency. *Phil.Trans. R. Soc. Lond. B* **355**, 473-489.

Kinosita, K., Jr., Adachi, K., and Itoh, H. (2004). Rotation of F_1-ATPase: how an ATP-driven molecular machine may work. *Annu. Rev. Biophys. Biomol. Struct.* **33**, 245–268.

Koshland, D. E. (1958). Application of a theory of enzyme specificity to protein synthesis. *Proc. Natl. Acad. Sci. USA* **44**, 98–104.

Menz, R. I., Walker, J. E., and Leslie, A. G. W. (2001). Structure of bovine mitochondrial F_1-ATPase with nucleotide bound to all three catalytic sites: implications for the mechanism of rotary catalysis. *Cell* **106**, 331-341.

Milgrom, Y. M., and Cross, R. L. (2005). Rapid hydrolysis of ATP by mitochondrial F_1-ATPase correlates with the filling of the second of three catalytic sites. *Proc. Natl. Acad. Sci. USA* **102**, 13831-13836.

Nishizaka, T., Oiwa, K., Noji, H., Kimura, S., Muneyuki, E., Yoshida, M., and Kinosita, K., Jr. (2004). Chemomechanical coupling in F_1-ATPase revealed by simultaneous observation of nucleotide kinetics and rotation. *Nat. Struct. Mol. Biol.* **11**, 142-148.

Noji, H., Yasuda, R., Yoshida, M., and Kinosita, K., Jr. (1997). Direct observation of the rotation of F_1-ATPase. *Nature* **386**, 299–302.

Noji, H., Bald, D., Yasuda, R., Itoh, H., Yoshida, M., and Kinosita, K. Jr. (2001). Purine but not pyrimidine nucleotides support rotation of F_1-ATPase. *J. Biol. Chem.* **276**, 25480-25486.

O'Neal, C. C., and Boyer, P. D. (1984). Assessment of the rate of bound substrate interconversion and of ATP acceleration of product release during catalysis by mitochondrial adenosine triphosphatase. *J. Biol. Chem.* **259**, 5761-5767.

Ono, S., Hara, K. Y., Hirao, J., Matsui, T., Noji, H., Yoshida, M., and Muneyuki, E. (2003). Origin of apparent negative cooperativity of F_1-ATPase. Biochim. Biophys. Acta 1607, 35-44.

Oosawa, F., and Hayashi, S. (1986). The loose coupling mechanism in molecular machines of living cells. *Adv. Biophys.* **22**, 151-183.

Rondelez, Y., Tresset, G., Nakashima, T., Kato-Yamada, Y., Fujita, H., Takeuchi, S., and Noji, H. (2005). Highly coupled ATP synthesis by F_1-ATPase single molecules. *Nature* **433**, 773-777.

Sakaki, N., Shimo-Kon, R., Adachi, K., Itoh, H., Furuike, S., Muneyuki, E., Yoshida, M., and Kinosita, K., Jr. (2005). One rotary mechanism for F_1-ATPase over ATP concentrations from millimolar down to nanomolar. *Biophys. J.* **88**, 2047-2056.

Shimabukuro, K., Yasuda, R., Muneyuki, E., Hara, K. Y., Kinosita, K., Jr., and Yoshida, M. (2003). Catalysis and rotation of F_1 motor: cleavage of ATP at the catalytic site occurs in 1 ms before 40° substep rotation. *Proc. Nat. Acad. Sci. USA* **100**, 14731-14736.

Shimabukuro, K., Muneyuki, E., and Yoshida, M. (2006). An alternative reaction pathway of F_1-ATPase suggested by rotation without 80°/40° substeps of a sluggish mutant at low ATP. *Biophys. J.* **90**, 1028-1032.

Shirakihara, Y., Leslie, A. G. W., Abrahams, J. P., Walker, J. E., Ueda, T., Sekimoto, Y., Kambara, M., Saika, K., Kagawa, Y., and Yoshida, M. (1997). The crystal structure of the nucleotide-free $\alpha_3\beta_3$ subcomplex of F_1-ATPase from the thermophilic *Bacillus* PS3 is a symmetric trimer. *Structure* **5**, 825-836.

Wang, H., and Oster, G. (1998). Energy transduction in the F_1 motor of ATP synthase. *Nature* **396**, 279-282.

Weber, J., Wilke-Mounts, S., Lee, R. S., Grell, E., and Senior, A. E. (1993). Specific placement of tryptophan in the catalytic sites of the *Escherichia coli* F_1-ATPase provides a direct probe of nucleotide binding: maximal ATP hydrolysis occurs with three sites occupied. *J. Biol. Chem.* **268**, 20126-20133.

Weber, J., and Senior, A. E. (2000). ATP synthase: what we know about ATP hydrolysis and what we do not know about ATP synthesis. *Biochim. Biophys. Acta* **1458**, 300-309.

Yasuda, R., Noji, H., Kinosita, K., Jr., and Yoshida, M. (1998). F_1-ATPase is a highly efficient molecular motor that rotates with discrete 120° steps. *Cell* **93**, 1117–1124.

Yasuda, R., Noji, H., Yoshida, M., Kinosita, K., Jr., and Itoh, H. (2001). Resolution of distinct rotational substeps by submillisecond kinetic analysis of F_1-ATPase. *Nature* **410**, 898–904.

Yasuda, R., Masaike, T., Adachi, K., Noji, H., Itoh, H., and Kinosita, K., Jr. (2003). The ATP-waiting conformation of rotating F_1-ATPase revealed by single-pair fluorescence resonance energy transfer. *Proc. Natl. Acad. Sci. USA* **100**, 9314-9318.

Yoshida, M., Muneyuki, E., and Hisabori, T. (2001). ATP synthase — a marvelous rotary engine of the cell. *Nat. Rev. Mol. Cell Biol.* **2**, 669-677.